Reversible Kinetics and Thermodynamics of the Homopolymerization of L-Lactide with 2-Ethylhexanoic Acid Tin(II) Salt

David R. Witzke* and Ramani Narayan

Department of Chemical Engineering, Michigan State University, East Lansing, Michigan 48824

Jeffrey J. Kolstad

Central Research, Cargill Incorporated, Minneapolis, Minnesota 55440

Received May 6, 1997; Revised Manuscript Received June 17, 1997[⊗]

ABSTRACT: The reversible kinetics of L-lactide bulk polymerization with tin(II) ethylhexanoate was determined over a wide range of temperatures, 130−220 °C, and monomer to initiator molar ratios, 1000−80 000. Both polymerization and depolymerization are accurately described by a reversible model with a propagation term that is first order in monomer and catalyst. The activation energy of propagation is 70.9 ± 1.5 kJ mol^{-1}. The enthalpy, entropy, and ceiling temperature of polymerization are -23.3 ± 1.5 kJ mol^{-1}, -22.0 ± 3.2 J mol^{-1} K^{-1}, and 786 ± 87 °C, respectively. Crystallization increases the propagation rate and decreases the apparent monomer equilibrium in proportion to the degree of crystallinity. Natural hydroxyl impurities stoichiometrically control the polymer molecular weight but do not significantly affect the propagation rate.

Introduction

Polylactide polymers and copolymers are currently receiving industrial attention for use as commodity resins.[1,2] Previously, polylactides were used primarily in biomedical applications. L-Lactic acid is produced by fermenting sugars derived from corn, potatoes, and other agricultural products. Polymer grade L-lactide is produced industrially by metal-catalyzed intramolecular transesterification of low molecular weight poly(L-lactic acid) (PLLA) in a solvent free, continuous process.[3] Poly(L-lactide) of controlled molecular weight is then produced continuously through the ring-opening polymerization of L-lactide in a moisture-free process. The relatively low heat of lactide polymerization compared to most industrial plastics (70−90 kJ/mol)[4] reduces the heat-transfer problems normally expected in bulk polymerization at large scale.[5] A preferred catalyst for lactide polymerization is 2-ethylhexanoic acid tin(II) salt. This catalyst is known for its fast rate of polymerization,[6,7] low degree of racemization at high temperature,[8,9] and acceptance by the FDA as a food additive.[7] The optimum catalyst level depends on the residence time of polymerization and the melt stability of the resin. In a moisture-rich environment the polylactide polymer of high molecular mass is thermodynamically unstable, as explained by the small equilibrium constant for the condensation reaction of lactic acid to poly(lactic acid).[5] Although the approach toward phase equilibrium between water and polymer is fast (adsorption),[5] the approach toward chemical equilibrium (hydrolysis) is sufficiently slow such that a shelf life can be defined for a particular resin or article.

Having intermediate glass transition temperatures, polylactides are amenable to chemical modification. The following capabilities permit the production of polylactide-based resins that vary widely in properties:[5] raising or lowering the glass transition temperature, producing either amorphous or semicrystalline polylactide, producing either a linear or branched molecular architecture. With controlled on-line racemization, both amorphous and semicrystalline polylactide copolymers can be produced with the same feedstock, catalyst, and continuous process.[3,5] These attributes along with good mechanical properties and processability, competitive cost, degradability, and compatibility with various forms of waste disposal, such as composting,[1,2] make polylactide copolymers attractive candidates for the supersession of single-use petroleum-based plastics.

High temperatures (170−220 °C) permit rapid polymerization with subsequent devolatilization and extrusion in the melt. However, at these temperatures the lactide equilibrium concentration in polymer is important and an irreversible kinetics model does not adequately describe the rate of polymerization. The devolatilization operation is critical after bulk polymerization where at least 3−5% lactide remains in the polymer. At these levels, the accumulation of lactide on resin processing equipment is a problem. Such high lactide levels would pose further problems in food contact applications where the extraction of lactide into food is a concern. Of additional importance is the quantification of the rate of depolymerization. This is important in postdevolatilization resin processing.

Although considerable work has been done on the mechanism of lactide polymerization with various catalysts,[7,9−24] only a few papers discuss the kinetics of lactide polymerization.[6,14,22,24] Of these, none address the reversible aspect of the polymerization. Using various catalysts and low temperatures, Dittrich and Schulz established that the rate of lactide conversion is first order in monomer and catalyst concentration.[22] Recent studies using aluminum alkoxide catalysts concur.[14,24] Eenink studied the kinetics of L-lactide bulk polymerization with tin(II) ethylhexanoate over a narrow temperature range, 103−130 °C.[6] He determined an activation energy for the propagation rate constant using an irreversible model that is first order in catalyst and monomer concentration.

We found few papers that addressed the thermodynamics of lactide polymerization. By measuring heat capacities and enthalpies of combustion, Kulagina et al.

[⊗] Abstract published in *Advance ACS Abstracts,* August 1, 1997.

S0024-9297(97)00631-1 CCC: $14.00

estimated the thermodynamic parameters of D,L-lactide copolymerization.[25] Duda and Penczek determined the thermodynamic parameters for L-lactide polymerization in dioxane, 80−133 °C, by measuring monomer equilibrium concentrations.[26] By extrapolation from solution data, they arrived at thermodynamic parameters for bulk polymerization.

In this study, kinetic experiments of L-lactide polymerization with tin(II) ethylhexanoate were performed over a wide range of temperatures (130−220 °C) and monomer to initiator molar ratios (1000−80 000). Depolymerization kinetics was also determined at these conditions using bulk devolatilized polymer. A monomer equilibrium curve was established, and the thermodynamics of L-lactide polymerization were quantified. These data were used to develop a reversible kinetic model for L-lactide polymerization with tin(II) ethylhexanoate that adequately predicts the rate of polymerization and depolymerization, over temperatures and catalyst concentrations of industrial interest. The effect of crystallization on the rate and extent of L-lactide polymerization was also quantitatively determined.

Experimental Section

Monomers. L- and D,L-lactide (racemate of D- and L-lactide) were purchased from Boehringer Ingelheim. Monomers were dried under vacuum for 12 h at 50 °C before polymerization. Gas chromatography, GC, was used to determine monomer purity. A Hewlett Packard 5890 GC was used: DB-17 capillary column (J&W), 30 m × 0.25 mm; 0.25 μm film thickness; injector (split, 100:1) at 200 °C; detector at 260 °C. Temperature program: 10 min at 100 °C, 10 °C/min to 250 °C, 3 min at 250 °C. Retention times: *meso*-lactide, 13.4 min; L-lactide and D-lactide, 14.6 min. Polylactide samples, along with internal standards, were dissolved in acetonitrile and reacted with a silane-based derivatizing reagent (*N*-methyl-*N*-(*tert*-butyldimethylsilyl)trifluoroacetamide with 1% *tert*-butyldimethylchlorosilane; Regis Chemical Co.) to enable the detection of acidic components. The L-lactide was 99.67% pure, with 0.24% *meso*-lactide, 0.072% lactoyllactic acid (DP2), 0.008% lactic acid, 0.008% DP3, and <0.005% DP4. The D,L-lactide was 99.71% pure, with 0.23% *meso*-lactide, 0.06% DP2, <0.005% lactic acid, and <0.005% DP3 plus DP4.

Catalyst. 2-Ethylhexanoic acid tin(II) salt (a.k.a. tin(II) ethylhexanoate, stannous octoate), 405.11 g/mol, was purchased from Aldrich. Reported purity is 95%, with 4.6% ethylhexanoic acid, 0.3−0.5% water, and less than 0.05% *tert*-butylcatechol (stabilizer). For transfer purposes, catalyst solutions (4−13% by weight) were prepared in anhydrous toluene (Aldrich). The catalyst solutions were prepared fresh for each polymerization.

Monomer Conversion Analysis. For conversions less than 90%, lactide concentration was determined by gel permeation chromatography, GPC. A Waters apparatus equipped with a 410 RI detector, 510 pump, equipped with three Ultrastyragel columns (in the order 10^5, 10^4, and 500 Å pore size), attached in series, was used. The analyses were performed at 35 °C using chloroform as eluent at a flow rate of 1 mL/min.

For conversions greater than 90%, extraction of lactide into cyclohexane with subsequent gas chromatography was used to determine the monomer concentration. GC is preferred at high conversion because low molecular weight degradation products become significant, in the time required to achieve high conversion, and coelute with the monomer during GPC. The polymer samples were dissolved into chloroform and further diluted with a larger volume of cyclohexane. The lactide isomers remain in solution while the polymer precipitates out and is removed by filtration. Internal standards were used with each run to verify the results. The same GC columns and temperature profile as with the monomer purity analysis were used. This GC lactide conversion method has an experimentally determined standard deviation of 0.012% lactide. Lactide levels as low as 0.005% are quantified.

Both the GPC and GC techniques for the determination of lactide concentration in polylactide have been extensively studied and verified by Cargill in a stringent safety assessment.[27]

Molecular Weight Determinations. Polylactide molecular weights were determined using the Waters GPC, calibrated against polystyrene standards. Polylactide molecular weights are reported relative to polystyrene standards and have not been corrected to an absolute basis using a universal calibration. The Mark−Houwink constants for polystyrene in chloroform at 35 °C were determined to be $K = 1.67 \times 10^{-4}$ dL/g and $a = 0.692$.

Water Analysis. A 684 KF coulometer by Brinkmann was used for the determination of water concentration in monomer before polymerization.

Degree of Crystallization. The crystalline melting temperature and heat of melting of the lactide polymers were determined by differential scanning calorimetry. A Mettler DSC 30 was used with a heating rate of 10 °C/min and sample sizes between 5 and 10 mg. The reported crystalline melting temperature corresponds to the temperature at which the maximum in the melting endotherm occurred. The heat of melting is reported as the integral of the melting endotherm. None of the tested samples crystallized during DSC operation, as noted by the absence of an exotherm in the DSC thermograms.

Density Measurements. The specific gravities of *meso*-lactide and L-lactide were measured in various hydrometers between 68 and 150 °C and 110 and 172 °C, respectively. The calibration of the hydrometers was verified with a Dow Corning oil having a well-known density.[5] The density of a devolatilized amorphous polylactide polymer was estimated between 150 and 210 °C using a capillary viscometer. Random, triplicate density estimations were made by measuring the weight of a displacement of polymer from a Haake Rosand RH7-2 capillary viscometer. The minor importance of the extensional flow components of polylactide allows for valid density values with this technique. The amorphous polymer was synthesized from 90% L-lactide and 10% *meso*-lactide.

Polymerization Procedure. Polymerizations were performed in the bulk in oven-dried, silanized, 8 and 40 mL vials. The polymer in the 40 mL vials was used for the depolymerization experiments. To obtain a uniform catalyst concentration in the vials, a mother flask was used to melt the monomer and add and mix the catalyst before transfer to the vials. Using a mineral oil bubbler, the flask was maintained under a slight pressure of dry nitrogen, passed through a molecular sieve indicating moisture and oxygen trap. The flask was evacuated and flushed with nitrogen several times with the use of a Firestone valve prior to monomer addition in a nitrogen-purged glovebag. Before catalyst addition, samples were taken for water and acidic impurity analysis. The catalyst solution was added through a septum inlet adapter by syringe. Once the catalyst was thoroughly mixed, the vessel was further pressurized with dry nitrogen, and the screw top vials were filled through a $^1/_4$ in. stainless steel sampling port under nitrogen flush.

The vials were then transferred to an adjacent silicon oil bath and immersed up to their caps with the use of a test tube rack to ensure isothermal polymerization. Temperature was controlled to within ±1 °C using autotuning PID controllers. Vials were pulled from the reaction bath at predetermined intervals, and the reactions were quenched by immersing the vials in liquid nitrogen. Molecular weight variability across a vial was determined by performing GPC on two vials sampled at four points each. The number-average molecular weight deviation was among 2−6% across each vial, which is comparable to the deviation for a single sample with repeat injection. We conclude that with this polymerization procedure there is no significant vial inhomogeneity. Polymerization samples at times less than 30 min were taken directly from the mother flask and transferred under nitrogen flush into 40 mL vials of chloroform, using 10 mL broken tip pipettes.

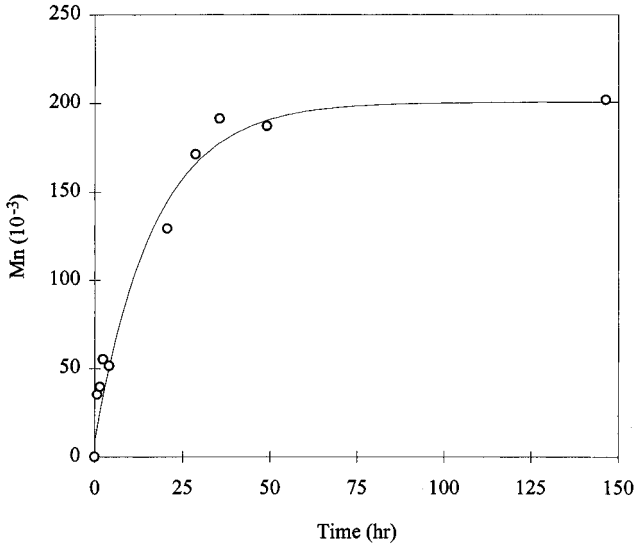

Figure 1. PLLA number-average molecular weight versus time. Polymerization conditions: 130 °C with a monomer to initiator ratio of 10 000.

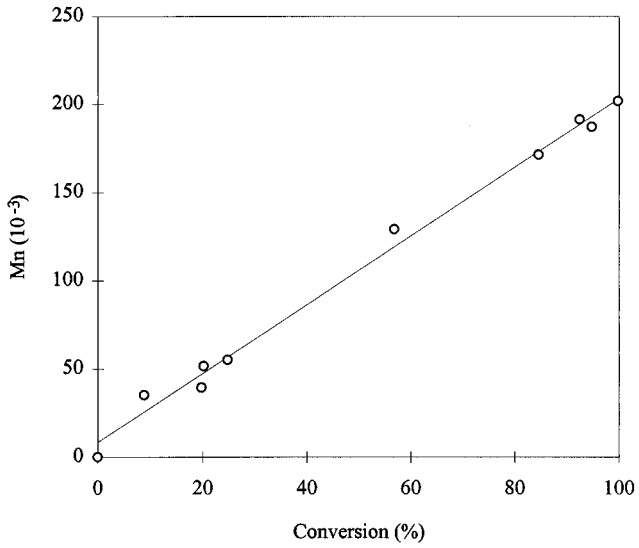

Figure 2. PLLA number-average molecular weight versus conversion. Polymerization conditions: 130 °C with a monomer to initiator ratio of 10 000.

Depolymerization Procedure. Residual lactide was removed from the polymers by reactive devolatilization. The polymer was ground to a powder, placed in aluminum trays at $^1/_4$ in. depth, and dried under vacuum for 4 h at 70 °C. The samples were heated to 160 °C and cooled under a nitrogen purge to 125 °C. The nitrogen line was closed, and the samples were exposed to a 0.5 mmHg vacuum for 12 h. Typical lactide levels after devolatilization were 0.01%. Devolatilized polymer samples were vacuum sealed with a propane torch in silanized 5 mL long-stem vacule ampules. Monomer reformation experiments were performed in insulated silicon oil baths with autotuning PID temperature controllers. At predetermined intervals, the vials were removed and quenched in liquid nitrogen for molecular weight and lactide concentration analyses.

Results and Discussion

Reversible Polymerization Model. Lactide polymerization data suggest a reversible rate form with a propagation term that is first order in monomer and catalyst. Figures 1 and 2 show representative curves of the change in number-average molecular weight with time and conversion. In agreement with Eenink[6] and Nijenhuis et al.,[23] initiation is fast compared to propagation. This was found at all polymerization conditions in this study. The linear dependence of molecular weight on conversion is consistent with a mechanism where initiation is fast, monomer does not react with monomer, and there is no termination of reaction centers. This type of molecular weight dependence is characteristic of living polymers and is typical with polymers from monomers possessing carboxyl electron-withdrawing groups.[4] Although the kinetics resemble anionic chain polymerization, the polymerization of lactide with tin(II) ethylhexanoate proceeds presumably through a coordination insertion mechanism.[7,9,11−19,24] Regardless of the mechanism, a general reversible rate form assuming fast initiation is proposed:

$$\mathrm{R}_n^* + \mathrm{M} \underset{k_d}{\overset{k_p}{\rightleftharpoons}} \mathrm{R}_{n+2}^* \qquad (1)$$

where lactide, M, is polymerized as lactic dimers on initiated polymer chains, R*. With the fairly well-established assumption of equal reactivity among functional groups and assuming that the total number of reaction centers is equivalent to the initial number of catalyst molecules, $I = \sum_{n=2}^{\infty} R_n^*$, the rate of polymerization is expressed as

$$\frac{-\mathrm{d}M}{\mathrm{d}t} = k_p MI - k_d I = k_p I(M - M_{eq}) \qquad (2)$$

The monomer equilibrium concentration, M_{eq}, is conveniently obtained from equilibrium experiments and is a function of temperature:

$$M_{eq} = \frac{k_d}{k_p} = \frac{1}{K_{eq}} = \exp\left(\frac{\Delta \mathrm{H}_{lc}}{RT} - \frac{\Delta S_{lc}}{R}\right) \qquad (3)$$

where ΔH_{lc}, ΔS_{lc}, and R are the heat of polymerization, entropy of polymerization, and gas constant, respectively. The subscripts in ΔH_{lc} and ΔS_{lc} refer to equilibrium between pure monomer liquid, l, and condensed amorphous polymer, c, as per the notation of Dainton and Ivin.[29] A complete thermodynamic description of reversible ring-opening polymerization is found elsewhere.[28−30] The propagation rate constant, k_p, depends on temperature and is described by an Arrhenius equation, where E_a is the activation energy and A_{448} is the preexponential constant referenced to 448 K,

$$k_p = A_{448} \exp\left(\frac{-E_a}{R}\left(\frac{1}{T(\mathrm{K})} - \frac{1}{448\ \mathrm{K}}\right)\right) \qquad (4)$$

Integrating eq (2) with an initial monomer concentration, M_0, gives the monomer concentration and conversion as a function of time:

$$M(t) = M_{eq} + (M_0 - M_{eq}) \exp(-k_p It) \qquad (5)$$

$$X_{mon}(t) = (1 - M_{eq}/M_0)(1 - \exp(-k_p It)) \qquad (6)$$

The four-parameter model defined by eqs 3, 4, and 6 simulates the extent of lactide polymerization and depolymerization as a function of time, temperature, catalyst concentration, and initial monomer concentration.

In the definition of the rate of lactide polymerization (eq 2) no account is taken for the volume change on reaction, i.e., $-\mathrm{d}M/\mathrm{d}t = (-\mathrm{d}M/\mathrm{d}t)_V$. Density data are presented in Figure 3. No statistical differences were

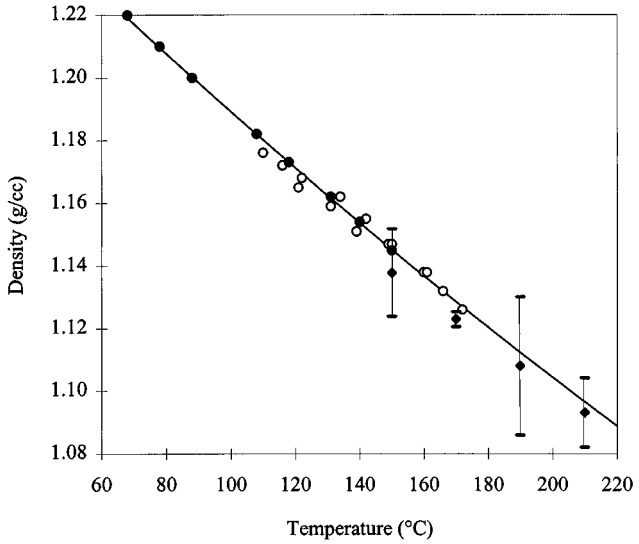

Figure 3. Liquid density versus temperature for *meso*-lactide (●), L-lactide (○), and amorphous polylactide (◆). The solid line is the density model defined by eq 7.

found among the liquid densities of *meso*-lactide, L-lactide, and amorphous polylactide at polymerization temperatures. Their densities were fit to a single-parameter model using a reference temperature of 150 °C, with a density of 1.145 g cm^{-3}. Between 68 and 172 °C, the thermal coefficient of expansion was determined to be 7.391×10^{-4} °C^{-1}. The melt densities, ρ, of lactide and amorphous polylactide are calculated using the following expression:

$$\rho(\text{g cm}^{-3}) = \frac{1.145}{1 + 0.0007391(T(°\text{C}) - 150)} \qquad (7)$$

The data suggest that the kinetic effect of the volume change on reaction is not significant.

In bulk ring-opening polymerizations where the change in volume on reaction can be neglected, it is appropriate to express equilibrium and non-first-order rate constants in terms of weight fractions. This is consistent with the fundamental correctness of using mole fractions to describe equilibrium constants in liquids.[31] Furthermore, weight fractions are common response variables for analytical measurements of monomer concentration in polymer, such as in GPC and GC. However, equilibrium constants for bulk ring-opening polymerizations are commonly expressed with units of concentration (molarity). Implicit in such data is an assumption of density and its temperature dependence, which makes it difficult to use published equilibrium data when good density data are unavailable at polymerization temperatures. In this work, weight fractions are used instead of concentrations, time is expressed in hours, and catalyst, I, is taken as the initial mole percentage. Expressed in this manner, the propagation rate constant has a magnitude of at least order unity with the dimensions h^{-1} catalyst mol %$^{-1}$. Equation 7 can be used to convert the equilibrium constant from a weight fraction to one having units of concentration.

Reversible Model Data Analysis. Using the reversible polymerization model, nonlinear regression analyses were performed on the polymerization and depolymerization kinetic data to determine the validity of the fitted model. Next, inferences about the effects of temperature and catalyst level are made. Finally, an analysis of predicted against observed conversion

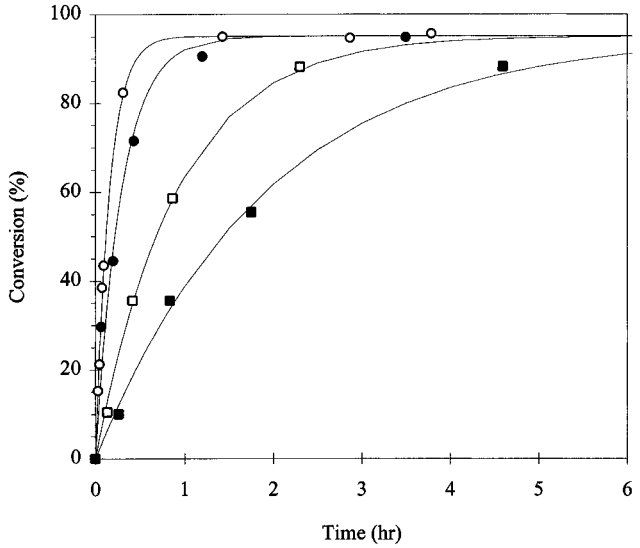

Figure 4. Effect of catalyst level on the kinetics of L-lactide polymerization at 220 °C. The solid lines are the reversible model fits for the respective monomer to initiator ratios: 10 100 (○); 20 000 (●); 39 600 (□); 79 300 (■).

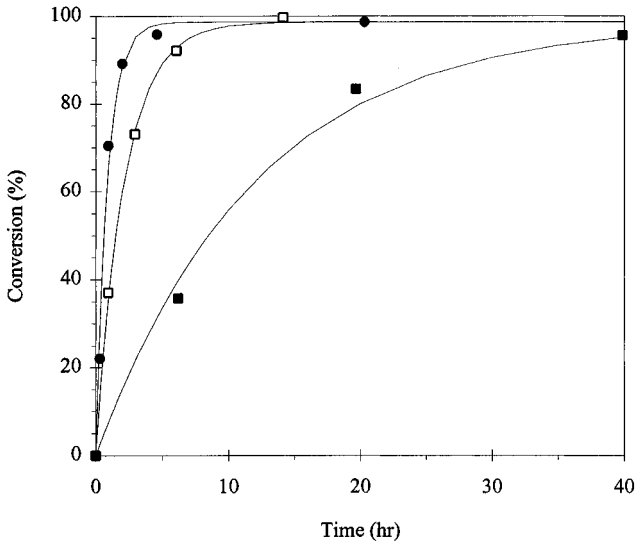

Figure 5. Effect of catalyst level on the kinetics of L-lactide polymerization at 130 °C. The solid lines are the reversible model fits for the respective monomer to initiator ratios: 1000 (●); 2940 (□); 19 200 (■).

was performed to determine the accuracy of the model among the temperatures and catalyst levels studied.

L-Lactide polymerization data at 220 °C, with molar ratios of monomer to initiator, M/I, varying between 10 000 and 80 000, are presented with the fitted model in Figure 4. Graphical analyses of the residuals confirmed that the propagation rate is first order in monomer. Figure 5 gives a visual assessment of the model's effectiveness at low temperature, 130 °C, and higher catalyst levels, M/I = 1000−20 000. The data are well represented by the model.

As a result of the reversibility of lactide polymerization, we can gain additional kinetic and thermodynamic information from depolymerization experiments. The regression of eq 6, with the appropriate value of M_0 for devolatilized polymer, gives a direct solution for k_p and M_{eq}. The propagation rate constant, k_p, and depropagation rate constant, k_d, are related through the equilibrium constant by the principle of microscopic reversibility (i.e., $M_{eq} = k_d/k_p$). It follows that catalysts that

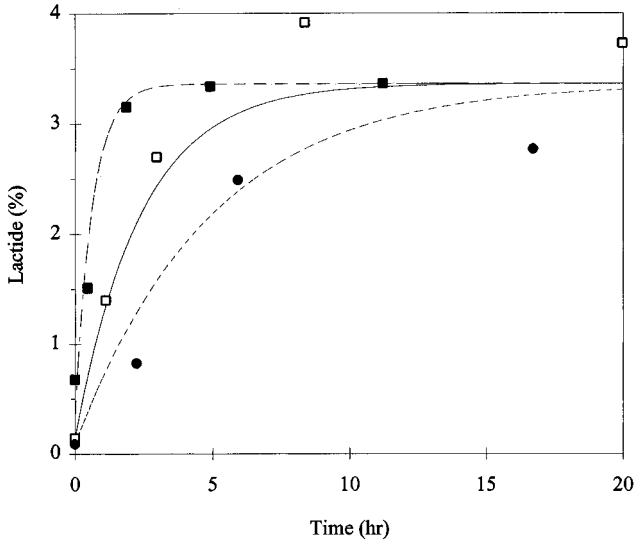

Figure 6. Effect of catalyst level on depolymerization of PLLA at 190 °C. The lines are the reversible model for the respective monomer to initiator ratios: (– –) for 10 300 (■); (—) for 39 200 (□); (---) for 80 600 (●).

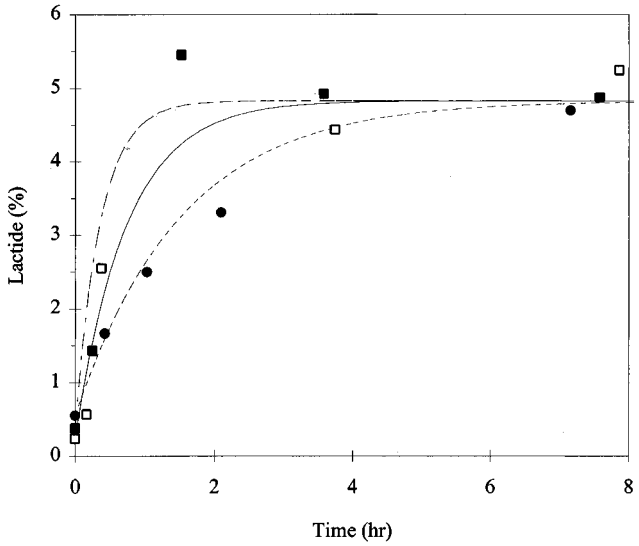

Figure 7. Effect of catalyst level on depolymerization of PLLA at 220 °C. The lines are the reversible model for the respective monomer to initiator ratios: (– –) for 19 200 (■); (—) for 39 200 (□); (---) for 80 600 (●).

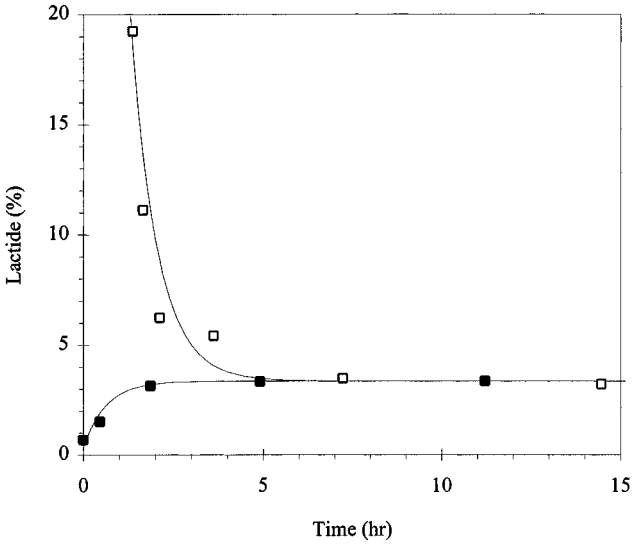

Figure 8. Approach toward chemical equilbrium at 190 °C. The solid line is the reversible model for the superimposed polymerization ((□) $M_0 = 1$, M/I = 10 000) and depolymerization ((■) $M_0 = 0.0068$, M/I = 10 300) data.

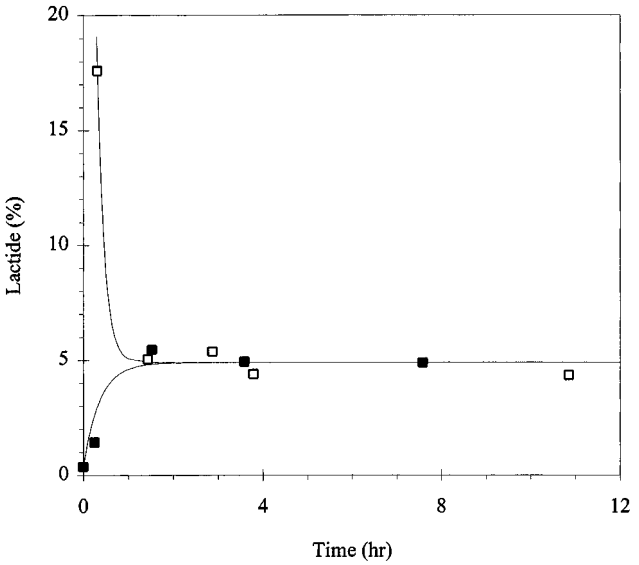

Figure 9. Approach toward chemical equilibrium at 220 °C. The solid line is the reversible model for the superimposed polymerization ((□) $M_0 = 1$, M/I = 20 000) and depolymerization ((■) $M_0 = 0.0038$, M/I = 19 200) data.

enable rapid polymerization should also give comparatively fast depolymerization. In this regard, it is not surprising that transesterification and hydrolysis are also catalyzed by lactide polymerization catalysts.[7,8,12,32]

The results of the depolymerization experiments at 190 and 220 °C are shown in Figures 6 and 7. Although scatter in the data is apparent, the data clearly show that the rate of depolymerization is dependent on catalyst concentration. As expected, there is no distinct trend between monomer equilibrium and catalyst level. Combining both polymerization and depolymerization data, Figures 8 and 9 show the approach toward chemical equilibrium. The reversible model fits the observed polymerization and depolymerization data well.

Racemization was found to be a significant side reaction during the 130–220 °C polymerization and depolymerization experiments. At conversions greater than 90%, the total lactide determined by GC contained between 2 and 20% *meso*-lactide. The initial *meso*-lactide amount before the polymerizations was 0.24%. The *meso*-lactide concentration in unreacted monomer increased with time and temperature. Monomer equilibrium concentrations are reported as the sum of lactide isomers.

The effect of temperature on polymerization is presented in Figure 10. At each temperature the propagation rate constant, k_p, and monomer equilibrium concentration, M_{eq}, were determined by nonlinear regression of eq 6. Likewise, k_p and M_{eq} values were determined for the depolymerization experiments. Direct nonlinear regression is preferred over linear regression because of the observed homogeneity of error in conversion versus time. A linear transformation of the conversion expression (eq 6) gives biased estimators upon regression, and an inferior fit is observed. The data from the polymerization and depolymerization experiments yielded consistent rate constant and equilibrium concentration estimates. However, the most precise estimates of k_p

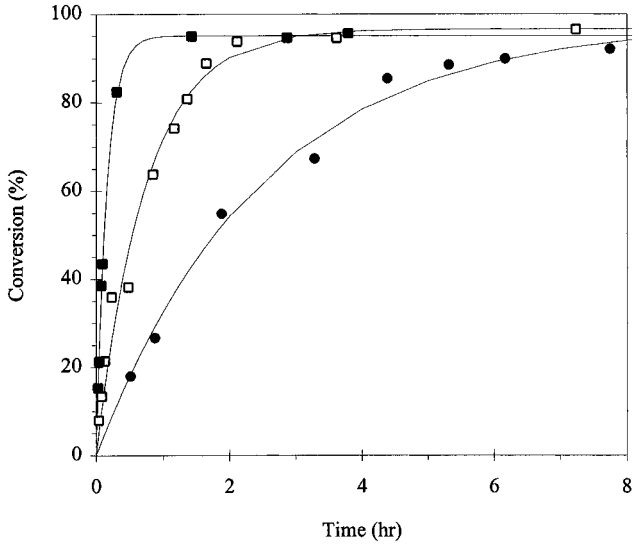

Figure 10. Effect of temperature on the kinetics of L-lactide polymerization with a monomer to initiator ratio of 10 000. The solid line is the reversible model for the respective temperatures: 220 °C (■), 190 °C (□), 160 °C (●).

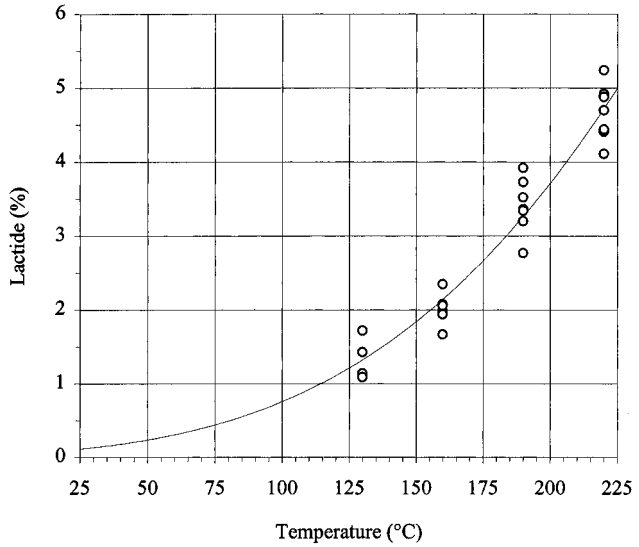

Figure 11. Monomer equilibrium curve for L-lactide polymerization (amorphous phase). The solid line is the equilbirium model defined in eq 3: $\Delta H_{lc} = -23.3$ kJ mol^{-1}, $\Delta S_{lc} = -22.0$ J mol^{-1} K^{-1}.

were obtained from polymerization data, and the most precise estimates of M_{eq} were obtained from depolymerization data. This is because more data were taken in the kinetically controlled portion of the curve for the polymerizations, while the depolymerization experiments tended to have more points in the equilibrium-sensitive portion of the curve.

An equilibrium curve of L-lactide in amorphous PLLA is shown in Figure 11. The monomer equilibrium values at 190 and 220 °C were determined from the depolymerization experiments. At 130 and 160 °C the M_{eq} were obtained from amorphous equilibrium data presented later, in Table 2. With a root-mean-square error of 0.33% lactide, the equilibrium lactide amounts at 130, 160, 190, and 220 °C were found to be 1.32, 2.15, 3.27, and 4.72 wt %, respectively. The heat and entropy of polymerization were determined by nonlinear regression of eq 3: $\Delta H_{lc} = -23.3 \pm 1.5$ kJ mol^{-1}, $\Delta S_{lc} = -22.0 \pm 3.2$ J mol^{-1} K^{-1}, from which, the ceiling temperature of polymerization ($\Delta G_{lc} = 0$) is estimated:

$$T_c = \frac{\Delta H_{lc}}{\Delta S_{lc}} = 786 \pm 87\ ^\circ\text{C} \qquad (8)$$

The calculated value of T_c is sensitive to the specified standard states: "pure" liquid monomer, amorphous polymer, 1 atm. The regression was performed using M_{eq} expressed in weight fractions; thus, the standard state $M = 1$ corresponds to pure liquid monomer. For bulk polymerization of L-lactide we believe T_c to be among 650−1038 °C (95% confidence limits). However, because the ceiling temperature lies well above nondepolymerization degradation temperatures,[33−37] T_c for lactide polymerization is hypothetical.

Thermodynamic parameters for the copolymerization of D,L-lactide were calculated from calorimetry data by Kulagina et al.[25] On the basis of comparable monomer equilibrium, we expect similar ΔH_{lc} and ΔS_{lc} values between polymers of L- and D,L-lactide. At 400 K Kulagina et al. estimated ΔH_{lc} and ΔS_{lc} at −27.0 kJ mol^{-1} and −13.0 J mol^{-1} K^{-1}, respectively. Although the enthalpies of polymerization are similar, the entropies differ significantly. Their values are referenced to a standard state of zero entropy for crystalline D,L-lactide at 0 K.

Duda and Penczek[26] reported thermodynamic parameters for L-lactide polymerization in 1,4-dioxane at temperatures from 80 to 133 °C. By extrapolating equilibrium data from solution to bulk concentrations, they arrived at the following parameters: $\Delta H_{lc} = -22.9$ kJ mol^{-1}, $\Delta S_{lc} = -25.03$ J mol^{-1} K^{-1} (T_c = 641 °C). Although their equilibrium data were determined in solution at low temperatures, the thermodynamic parameters lie within the standard error of our estimates. In accordance with the data of Duda and Penczek, we feel our thermodynamic parameters accurately describe the chemical equilibrium between L-lactide and amorphous PLLA.

After establishing the equilibrium relationship, propagation rate constants were regressed from the polymerization data using the reversible model. A summary of the results is presented in Table 1. Although crystallization accompanied polymerization at 130 °C, the propagation rate constants reported in Table 1 are independent of the influence of crystallization on the polymerization rate. The rate constants at 130 °C were regressed using the reversible model at the predetermined amorphous monomer equilibrium amount of 1.32%. Good model fits were obtained for the 130 °C rate data at conversions less than 50%. These k_p are in good agreement with k_p determined from the irreversible model using rate data at less than 50% conversion. A discussion and model of the effect of crystallization on the rate of polymerization are presented later in this paper.

The rate equation assumption of first-order dependence on I was verified by fitting the data to a power law rate form: $k_{eff} = kI^{\alpha}$, where $k_{eff} = k_p I$. Regression of the 220 °C data gave $\alpha = 1.10 \pm 0.14$. A similar analysis was performed on the 220 °C depolymerization data (Figure 7), yielding $\alpha = 0.76$. However, because of variance in the depolymerization data, the 95% confidence limits on α are 0.26 and 1.50. Therefore, the rates of lactide propagation and depropagation with tin(II) ethylhexanoate are indeed first order in catalyst.

The temperature dependence of k_p is depicted with an Arrhenius plot in Figure 12. Using all the polymerization data, the activation energy and preexponential constant were determined by nonlinear regression with

Table 1. Propagation Rate Constant Summary

T (°C)	M/I (mol/mol)	I (mol %)	k_p (h^{-1} catalyst mol $\%^{-1}$)
130	1 000	0.0999	11.3
130	2 940	0.0340	13.8
130	9 460	0.0106	6.1
130	19 200	0.00522	16.0
160	9 890	0.0101	40.1
190	10 000	0.0100	136
220	10 100	0.00993	639
220	20 000	0.00500	687
220	39 600	0.00253	435
220	79 300	0.00126	416

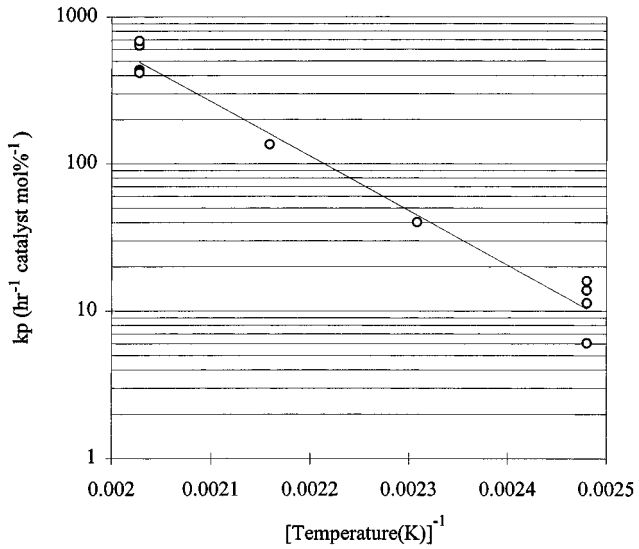

Figure 12. Temperature dependence of the propagation rate constant of L-lactide with tin(II) ethylhexanoate. The solid line is the Arrhenius model defined in eq 4: $E_a = 70.9$ kJ mol^{-1}, $A_{448} = 86.0$ h^{-1} catalyst mol %$^{-1}$.

eqs 4 and 6: $E_a = 70.9 \pm 1.5$ kJ mol^{-1}, $A_{448} = 86.0 \pm 3.0$ h^{-1} cat mol %$^{-1}$. Thus, the propagation rate constant can be estimated over a large temperature range using eq 4.

Eenink[6] calculated an activation energy of 80.6 kJ mol^{-1} for L-lactide polymerization with tin(II) ethylhexanoate, M/I = 10 000, from 103 to 130 °C, using an irreversible rate model that is first order in catalyst and monomer. Eenink regressed his data at conversions far from equilibrium (less than 85%), and any error in his calculated rate constants attributed to the irreversibility of the model is small. The minor discrepancy in activation energy may be attributed to the increased variance in E_a with the narrow temperature range.

The effect of model choice on the rate constant is described in Figure 13. From eq 5, a plot of $-\ln((M - M_{eq})/(M_0 - M_{eq})) = kIt$ versus time should be linear. The equivalent expression for the irreversible model is $-\ln(M/M_0) = kIt$. Thus, the slope of these curves is the propagation rate constant for the respective model. At low temperatures, such as those used in the Eenink study, the rate constant is fairly insensitive to time at conversions less than 85%. At higher conversions the apparent rate constant decreases until a value of zero is arrived at equilibrium. At industrial temperatures (>180 °C), the effect of equilibrium on the apparent rate constant becomes more dramatic at lower conversions and the irreversible model is less adequate. With our data, plots of $-\ln((M - M_{eq})/(M_0 - M_{eq}))$ versus time yield straight lines over all conversion.

On account of decreasing polymerization rates, Eenink[6] found the irreversible fit poor for conversions

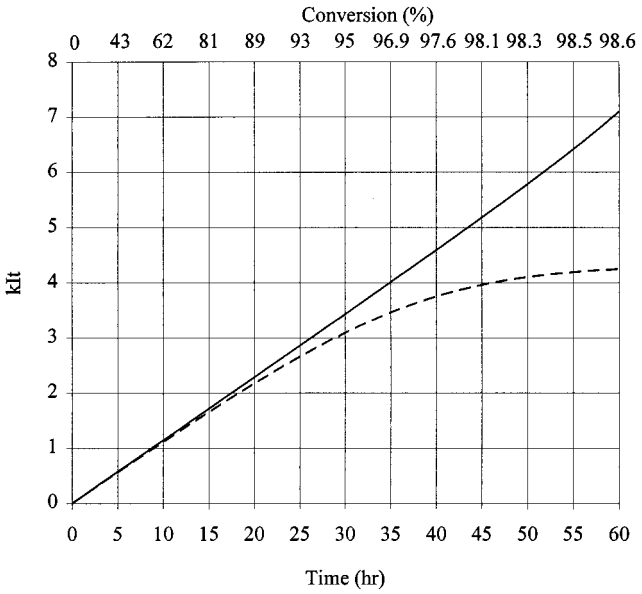

Figure 13. Effect of model choice on the observed L-lactide polymerization rate constant at 130 °C and M/I = 10 000. The slopes of these lines are the respective rate constants. The solid line is the reversible model, whereas the dashed line represents the irreversible model.

greater than 85%. In a similar finding, Nijenhuis et al.[23] suggested that L-lactide polymerized with tin(II) ethylhexanoate becomes diffusion controlled at conversions greater than 80%. The polymerizations in both contributions were performed at temperatures where crystallization accompanied polymerization. However, this same result was also reported for amorphous poly(D,L-lactide) by Lyudvig et al.,[38,39] who attributed the decreasing rates to a "gel effect" resulting from hydrogen bonding.[38] On the basis of the thermodynamic calculations of Kulagina et al.,[25] which infer from free energy calculations that at $T < 200$ °C the monomer equilibrium amount is less than 0.5%, Eenink discounted the influence of equilibrium on the rates. However, direct measurements in our work conclude that monomer equilibrium is of greater consequence and suggest that some of the decreases found in polymerization rates at high conversion may be attributed to chemical equilibrium.

The reversible model accurately predicts the kinetics of the reversible polymerization of L-lactide with tin(II) ethylhexanoate among 130−220 °C with M/I = 1000−80 000, over a full range of conversion. The incorporation of temperature transforms the model from one that has two parameters, k_p and M_{eq}, into one that has four: A, E_a/R, $\Delta H_{lc}/R$, and $\Delta S_{lc}/R$. A diagnostic plot of predicted lactide amounts versus observed amounts for the polymerization data is presented in Figure 14. The plot yields points that appear randomly distributed about the 45° line and exhibit no distinct pattern. At conversions less than 85%, the root-mean-square error of the model, RMSE, is 5.7% lactide. Above 85% conversion and at equilibrium the RMSE's are 1.5% and 0.33% lactide, respectively. Figure 15 shows the effectiveness of the model for predicting depolymerization. The model predicts the depolymerization data with a RMSE of 0.38% lactide. In summary, the plots confirm the appropriateness of the reversible model and the fit of the kinetic data.

Effect of Crystallization on Polymerization. Crystallization accompanies the bulk polymerization of L-

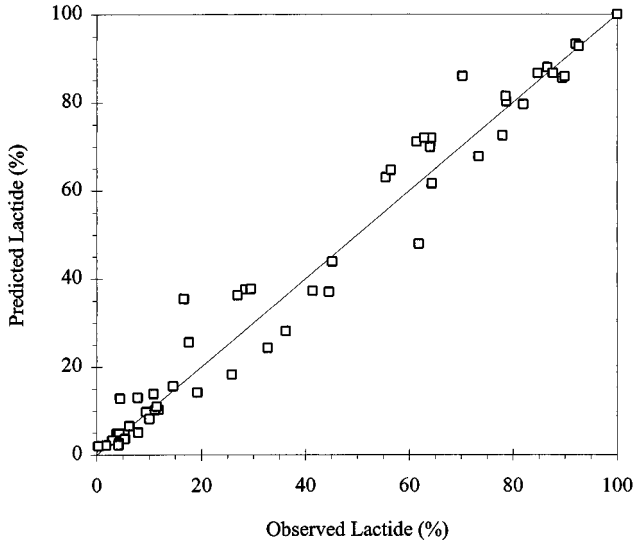

Figure 14. Reversible model performance for the L-lactide polymerization data. Polymerization conditions: 130−220 °C, M/I = 1000−80 000. The root-mean-square error of the model is 5.7% lactide.

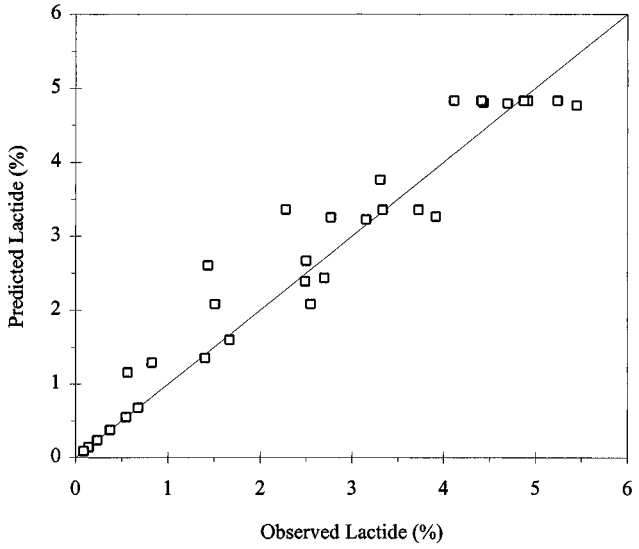

Figure 15. Reversible model performance for the L-lactide depolymerization data. Depolymerization conditions: 190−220 °C, M/I = 10 000−80 000. The root-mean-square error of the model is 0.38% lactide.

lactide at temperatures between 100 and 145 °C. From our 130 °C polymerization and depolymerization data, we found that crystallization increases the polymerization rate and decreases the total amount of monomer at reaction equilibrium. These results are in accord with the data of Nijenhuis et al.[23] To quantify the effects of crystallization, we assume that only functional groups in the amorphous phase remain available for reaction and that catalyst and lactide monomer are rejected from the polymer crystalline phase.

Depolymerization experiments at 130 and 160 °C with highly crystalline poly(L-lactide) yielded equilibrium lactide concentrations that were lower than expected based on the 190 and 220 °C results. During these experiments the PLLA melting temperature was above the test temperature, and the samples remained as loose powders. Thus, the depolymerization reaction appears to be excluded from the crystalline phase; consequently, the total lactide concentration in the polymer is suppressed.

Table 2. Monomer Equilibrium at 160 and 130 °C

composition[a] (L)	T (°C)	lactide (%)	M_n
50	160	1.99	84 600
50	160	2.08	107 800
85	160	1.94	78 700
85	160	1.67	85 200
100	160	2.35	76 800
100	160	2.06	70 500
50	130	1.43	99 600
50	130	1.72	122 800
85	130	1.14	87 600
85	130	1.09	94 700
100	130	0.16[b]	88 400
100	130	0.43[b]	88 900

[a] Remainder of D-lactide. [b] Semicrystalline.

Table 3. Crystallization of Poly(L-Lactide) during Polymerization at 130 °C, M/I = 9500

time (h)	conversion (%)	ΔH_m (J/g)	ω	T_m (°C)
2.37	13.3	0	0	
4.23	20.0	20.0	0.21	125.0
8.82	39.2	*a*	*a*	*a*
15.4	64.0	26.5	0.28	138.2
24.1	81.0	46.9	0.50	156.0
28.8	90.5	*b*	*b*	173.7
45.5	97.75	82.9	0.88	184.0
49.5	98.30	79.1	0.84	186.3
146	99.79	83.7	0.89	197.6

[a] Not determined. [b] Poor DSC thermogram; allowed detection of T_m only.

This hypothesis, based on depolymerization data, was confirmed through polymerization tests. According to the hypothesis, a noncrystallizable random copolymer of L- and D-lactide should retain a higher lactide concentration than a crystalline polylactide. Table 2 shows the equilibrium lactide values for long time polymerizations at 130 °C (24 h) and 160 °C (5 h), M/I = 1000, with three isomer compositions: 50%, 85%, and 100% L-lactide (with D-lactide as the balance). Lactic acid was used to stoichiometrically control the number-average molecular weights at 85 000. At 160 °C all the polymerizations proceeded in the absence of crystallization, and no statistical differences in monomer equilibrium were found among the three isomer compositions. However, at 130 °C the 100% L polymers crystallized during polymerization, and the total amounts of lactide in these semicrystalline samples were substantially reduced. Therefore, crystallization reduces the apparent equilibrium monomer concentration in polylactide.

Along with the lactide equilibrium effect, crystallization also affects lactide polymerization kinetics. With our 130 °C L-lactide polymerization data, plots of $-\ln((M - M_{eq})/(M_0 - M_{eq}))$ versus time yield a propagation rate constant (the slope) that increases with time. Thus, the reversible model is no longer valid when crystallization accompanies polymerization.

Table 3 presents a summary of the 130 °C polymerization data with M/I = 9500. Polymer crystallinity was found in quenched samples with conversions greater than 20%. Somewhere between 20 and 60% conversion the polymer began to crystallize and precipitate out of solution. This corresponds to the point where the melting temperature, T_m, exceeded the polymerization temperature. Differential scanning calorimetry was used to determine T_m and heat of melting, ΔH_m. The crystalline weight fractions, ω, were obtained by dividing the heats of melting by 93.7 J/g, the approximate heat of melting at 100% crystallinity determined by Fischer et al.[40] from single crystals of PLLA.

The melting point and heat of melting were found to increase with time. The final sample had a heat of melting of 83.7 J/g and a T_m of 197.6 °C. The 14 °C increase in melting point observed over the last 2% conversion is likely because of an annealing process, 100 h at 130 °C.

It is noteworthy that Nijenhuis et al.[23] obtained an as-polymerized PLLA heat of melting of 100 J/g, T_m = 207 °C, using a zinc catalyst. From observed T_m versus crystallization temperature data, Vasanthakumari and Pennings[41] extrapolated a theoretical PLLA melting temperature of 207 °C.

The instantaneous monomer and catalyst concentrations in the amorphous phase increase when polymer crystallizes and precipitates out of solution. Thus, if both catalyst and monomer are excluded from the crystalline phase, it follows that the rate of polymerization should subsequently increase. With these assumptions the open system mass balance on monomer weight fraction in the amorphous phase, M, is

$$dM = -k_p I M\, dt + k_d\, I\, dt - M\frac{dV}{V} \tag{9}$$

where V is the volume in the amorphous phase, and I, k_p, and k_d are the mole percentage catalyst, propagation constant, and depropagation constant, respectively.

The assumption of catalyst exclusion from the crystalline phase is justified by assuming that the catalyst concentration in the amorphous phase remains constant during crystallization (incorporation into the crystals without differentiation). For instantaneous crystallization of formed polymer, $M = 1$ and $dM = 0$, eq 9 gives a polymerization rate that is not significantly different from the reversible model at 130 °C (eq 5; this solution is identical to eq 5 when $M_{eq} = 0$ (irreversible). Thus, if the catalyst concentration remains constant, crystallization does not affect the apparent rate of monomer conversion. From our polymerization data, which clearly show that crystallization increases the rate of polymerization, we conclude that the catalyst must be excluded from the crystalline phase: $I(t) = V_0 I_0 / V(t)$.

The following equation relates the volume in the amorphous phase, the weight fraction of the crystalline phase, ω, and the ratio of the apparent (measured) monomer weight fraction to the amorphous phase monomer weight fraction:

$$\frac{V(t)}{V_0} = 1 - \omega(t) = \frac{M(t)_{apparent}}{M(t)} \tag{10}$$

Using eq 10, the chain rule, $dM_{apparent} = (V/V_0)\, dM + (M/V_0)\, dV$, and eq 9 incorporating the definition for $I(t)$, the mass balance for the apparent monomer weight fraction is

$$dM_{apparent} = (M_{eq} - M) k_p I_0\, dt \tag{11}$$

where M_{eq} is the equilibrium monomer weight fraction in the amorphous phase (eq 3).

Equation 11 can only be solved if we know how $M_{apparent}$ changes with respect to M (i.e., we have crystallization kinetics). However, we can directly solve for the lower bound of $M(t)_{apparent}$ by assuming instantaneous crystallization of polymer, $M = 1$. Integrating between $M_{0,apparent}$ and $M(t)_{apparent}$, we find that with instantaneous crystallization the apparent monomer weight fraction is a linear function of time.

$$M(t)_{apparent} = M_{0,apparent} + (M_{eq} - 1) k_p I_0 t \tag{12}$$

For unknown crystallization kinetics we assume an empirical relationship between $M_{apparent}$ and M to solve eq 11. A well-behaved family of curves is obtained by using the relationship

$$M = M_{apparent}^{1-\alpha} \tag{13}$$

where $0 \le \alpha \le 1$. When $\alpha = 0$, polymerization proceeds in the absence of crystallization and the solution to eq 11 is equivalent to the reversible model, $M_{apparent} = M$. When $\alpha = 1$, the solution of eq 11 yields the instantaneous crystallization solution (eq 12). The analytical solution to eq 11 is simplified by assuming irreversible kinetics, $M_{eq} = 0$. The error in doing this is negligible, except at apparent conversions near 100% where the relative error becomes large.

$$M(t)_{apparent} = (M_{0,apparent}^{\alpha} - \alpha k_p I_0 t)^{1/\alpha} \tag{14}$$

The family of curves for different α are presented in Figure 16 along with the observed 130 °C polymerization data. With $\alpha = 0.4$ an adequate fit of the kinetic data is observed. The α parameter can be directly obtained from crystallization and conversion data; $M(t)_{apparent} = (1 - \omega(t))^{1/\alpha}$. A value of $\alpha = 0.4$ also adequately fits the crystallinity data.

The effect of crystallinity on the depolymerization of L-lactide at 160 °C, M/I = 9500, is shown in Figure 17. In 16 h the monomer in the highly crystalline sample, $\omega = 0.89$, increased from 0.004% to only 0.26%. In contrast, the reversible model predicts that amorphous polylactide would obtain a M_{eq} of 2.15%. This is consistent with the measured value of 0.26% if all the lactide is in the amorphous phase. The apparent monomer concentration at reaction equilibrium can be determined from the product of the amorphous weight fraction and the known equilibrium concentration in the amorphous phase (eq 3).

$$M_{eq,apparent} = (1 - \omega) M_{eq} \tag{15}$$

We conclude that crystallization increases the rate of polymerization and decreases the apparent monomer equilibrium concentration in proportion to the degree of crystallinity. Furthermore, polymerization and depolymerization rate data are consistent with a process where reaction only occurs in the amorphous phase and catalyst and lactide monomer are excluded from the crystalline phase.

Effect of Natural Hydroxyl Impurities on the Kinetics of Lactide Polymerization. Natural impurities in lactide include lactic acid, lactoyllactic acid (DP2), DP3, DP4, and water. Oligomers larger than DP4 are not detectable with our GC protocol (less than 0.005%). It is known that hydroxyl impurities stoichiometrically control the number-average molecular weight of polylactide.[3,9,12,23,42] Each of the hydroxy acid impurities or water, which serve to initiate a polymer chain, is expected to form a polymer chain with one hydroxyl end group and one acid end group. The linearity of a plot of number-average molecular weight versus conversion (Figure 2) indicates that no significant intermolecular condensation reactions occur between the hydroxyl and the acid end groups.

In this study, the number-average molecular weights were usually controlled to less than 95 000 to facilitate

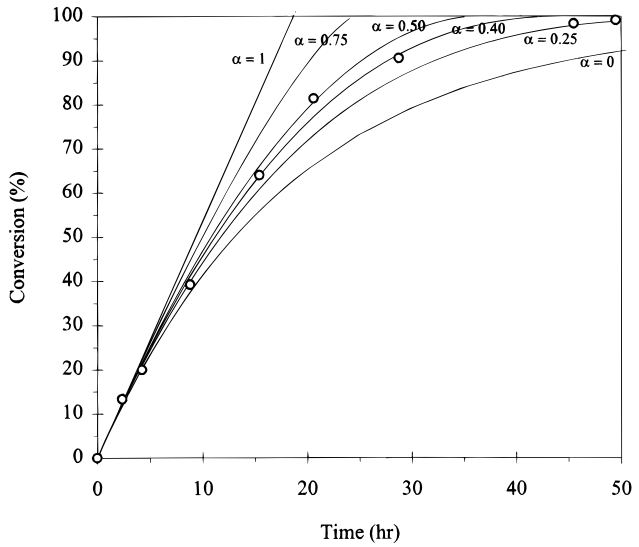

Figure 16. Effect of crystallization on the kinetics of L-lactide polymerization at 130 °C with M/I = 9500. The solid lines are the family of curves defined by eq 14 for various α. The observed data are represented by ○. For α = 0, no crystallization, the curve is equivalent to the reversible model (eq 6). For α = 1, instantaneous crystallization of polymer, the curve is equivalent to the analytical solution presented in equation 12.

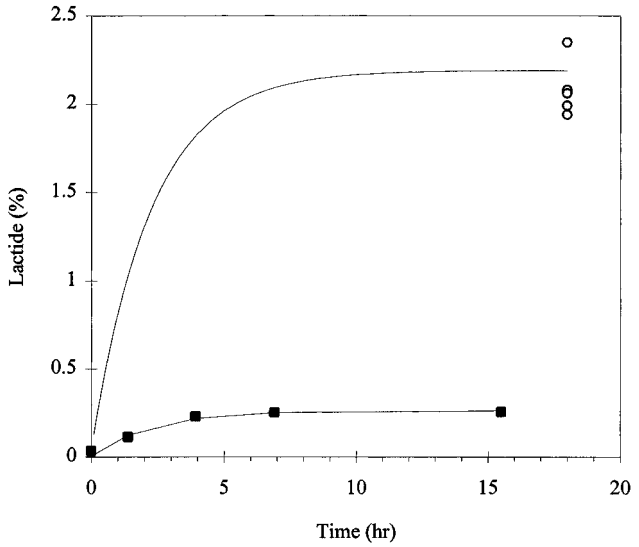

Figure 17. Effect of crystallization on the depolymerization kinetics of PLLA (■) at 160 °C with M/I = 10 000. The sample had a heat of melting of 83.7 J/g, $\omega = 0.89$. The upper solid line is the reversible model. Equilibrium L-lactide polymerization data at 160 °C (amorphous) is presented for reference (○).

grinding of the polymer. Our experience using lactic acid to control molecular weight indicates that natural impurities do not significantly affect the rate of polymerization to high polymer. For example, at 130 °C and M/I =10 000, we used lactic acid to target molecular weights between 87 000 and 201 000 in three polymerizations. Analyses of the kinetic data gave propagation rate constants that were not statistically different. Furthermore, from the depolymerization data we found no correlation between monomer equilibrium and molecular weight.

It is conceivable, however, that at low molecular weights (i.e., high level of impurities) the rates of propagation and depropagation are influenced by the higher concentration of hydroxyl end groups. Therefore,

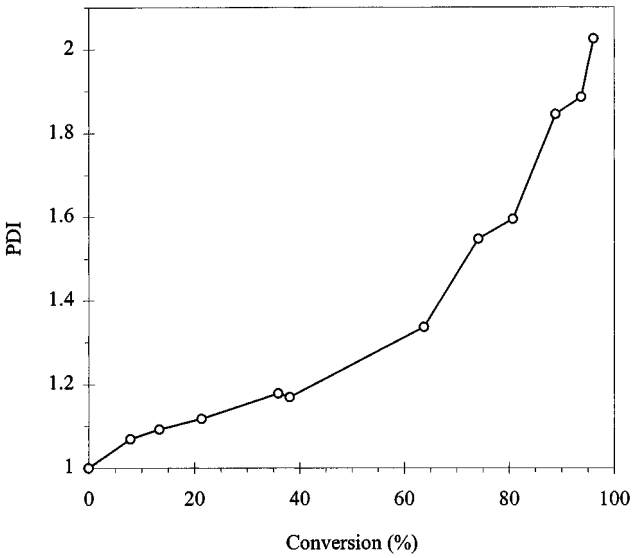

Figure 18. Plot of polydispersity index versus L-lactide conversion at 190 °C and M/I = 10 000. Transesterification reactions are responsible for the approach of PDI toward 2.0 (most probable distribtion).

we cannot conclude from our data that natural hydroxyl impurities do not mechanistically influence the polymerization kinetics of lactide with tin(II) ethylhexanoate. However, it is clear that, in the polymerization to high polymer, the relative importance of catalyst concentration and temperature renders any kinetic effects of natural impurities insignificant.

Tin(II)-catalyzed intermolecular transesterification among polymer chains (interchange reactions) yields a polymer molecular mass that approaches the most probable distribution.[5] The total amount of hydroxyl end groups is conserved throughout the polymerization; thus, the natural impurities determine the final molecular weight of the polymer. We found that with high polymerization temperatures, ≥160 °C, a polydispersity index (PDI = M_w/M_n) of 2.0 is achieved. The approach of PDI to 2.0 at 190 °C is presented in Figure 18. However, with our 130 °C data we found transesterification to be "incomplete" at equilibrium conversion, PDI = 1.5−1.6. This is in accord with Eenink:[6] PDI = 1.6 at 130 °C.

We conclude that natural hydroxyl impurities are not kinetically limiting in the propagation step and suggest that they do not participate in termination reactions with reactive centers. For these reasons, the kinetic rate form of polymerization is consistent with a living polymerization. However, the hydroxyl impurities do participate in transesterification reactions that broaden the molecular weight distribution and define the molecular mass of the polymer.

Conclusions

The proposed model describes the reversible polymerization kinetics of L-lactide with tin(II) ethylhexanoate over a wide range of temperatures and catalyst concentrations. Crystallization increases the propagation rate and decreases the apparent monomer equilibrium concentration—the amorphous phase monomer equilibrium remains unchanged. In addition, natural hydroxyl impurities were measured and found not to kinetically influence monomer conversion. However, these impurities stoichiometrically control the polymer molecular weight.

Acknowledgment. We gratefully acknowledge the suggestions and constructive criticisms provided by Eric Grulke. Thanks are due to Kris Butts for assisting in the density measurements. We are also very much indebted to colleagues at Cargill for their analytical expertise, particularly, Eric Hall and Karl Ludescher. We thank Cargill Incorporated for support of this research.

References and Notes

(1) McCarthy-Bates, L. *Plast. World* **1993**, March.
(2) Dean, K., Ed. *Ind. Bioprocess.* **1993**, *15*, No. 11.
(3) Gruber, P. R.; Hall, E. S.; Kolstad, J. J.; Iwen, M. L.; Benson, R. D.; Borchardt, R. L. (Cargill). U.S. Patent 5142023, 1992.
(4) Odian, G. *Principles of Polymerization*, 3rd ed.; John Wiley & Sons: New York, 1991.
(5) Witzke, D. R. Introduction to Properties, Engineering, and Prospects of Polylactide Polymers. Ph.D. Dissertation, Michigan State University, East Lansing, MI, 1997.
(6) Eenink, M. J. D. Synthesis of Biodegradable Polymers and Development of Biodegradable Hollow Fibres for the Controlled Release of Drugs. Ph.D. Thesis, Technische Hogeschool Twente Enschede, Enschede, The Netherlands, 1987.
(7) Leenslag, J. W.; Pennings, A. J. *Makromol. Chem.* **1987**, *188*, 1809.
(8) Kricheldorf, H. R.; Serra, A. *Polym. Bull.* **1985**, *14*, 497.
(9) Kricheldorf, H. R.; Sumbel, M. *Eur. Polym. J.* **1989**, *25*, 585.
(10) Johns, D. B.; Lenz, R. W. In *Ring-Opening Polymerization*; Ivin, K. J., Saegusa, T., Eds.; Elsevier Applied Science Publishers: London, 1984; Vol. 1, p 461.
(11) Kricheldorf, H. R.; Kreiser-Saunders, I.; Scharnagl, N. *Makromol. Chem. Macromol. Symp.* **1990**, *32*, 285.
(12) Dahlmann, J.; Rafler, G. *Acta Polym.* **1993**, *44*, 103.
(13) Kricheldorf, H. R.; Boettcher, C. *Makromol. Chem.* **1993**, *194*, 1653.
(14) Dubois, Ph.; Jacobs, C.; Jerome, R.; Teyssie, Ph. *Macromolecules* **1991**, *24*, 2266.
(15) Kohn, F. E.; van Ommen, J. G.; Feijen, J. *Eur. Polym. J.* **1983**, *19*, 1081.
(16) Dubois, Ph.; Jerome, R.; Teyssie, Ph. *Makromol. Chem., Macromol. Symp.* **1991**, *42/43*, 103.
(17) Kricheldorf, H. R.; Berl, M.; Scharnagl, N. *Macromolecules* **1988**, *21*, 286.
(18) Kricheldorf, H. R.; Sumbel, M. V.; Kreiser-Saunders, I. *Macromolecules* **1991**, *24*, 1944.
(19) Dubois, Ph.; Jerome, R.; Teyssie, Ph. *Polym. Bull.* **1989**, *22*, 475.
(20) Kricheldorf, H. R.; Kreiser-Saunders, I. *Makromol. Chem.* **1990**, *191*, 1057.
(21) Kricheldorf, H. R.; Dunsing, R. *Makromol. Chem.* **1986**, *187*, 1611.
(22) Dittrich, W.; Schulz, R. C. *Makromol. Chem.* **1971**, *15*, 109.
(23) Nijenhuis, A. J.; Grijpma, D. W.; Pennings, A. J. *Macromolecules* **1992**, *25*, 6419.
(24) Barakat, I.; Dubois, Ph.; Jerome, R.; Teyssie, Ph. *J. Polym. Sci., Part A: Polym. Chem.* **1993**, *31*, 505.
(25) Kulagina, T. G.; Lebedev, B. V.; Kiparisova, Ye. G.; Lyudvig, Ye. B.; Barskaya, I. G. *Polym. Sci. U.S.S.R.* **1982**, *24*, 1702.
(26) Duda, A.; Penczek, S. *Macromolecules* **1990**, *23*, 1636.
(27) Eichen Conn, R.; Kolstad, J. J.; Borzelleca, J. F.; Dixler, D. S.; Filer, L. J., Jr.; LaDu, B. N., Jr.; Pariza, M. W. *Food Chem. Toxicol.* **1995**, *33*, No. 4, 273.
(28) Ivin, K. J. *Encyclopedia of Polymer Science and Technology*; Wiley: New York, 1977; Suppl. Vol. 2, p 700.
(29) Dainton, F. S.; Ivin, K. J. *Quart. Rev. Chem. Soc.* **1958**, *12*, 61.
(30) Ivin, K. J. In *Polymer Handbook*, 2nd ed.; Brandrup, J.; Immergut, E. H., Ed.; Interscience: New York, 1975; p II 241.
(31) Allen, P. E. M.; Patrick, C. R. *Kinetics and Mechanisms of Polymerization Reactions*; Horwood: Chichester, U.K., 1974.
(32) Zang, X.; Wyss, U. P.; Pichora, D.; Goosen, M. F. A. *Polym. Bull.* **1992**, *27*, 623.
(33) McNeill, I. C.; Leiper, H. A. *Polym. Degrad. Stab.* **1985**, *11*, 267.
(34) McNeill, I. C.; Leiper, H. A. *Polym. Degrad. Stab.* **1985**, *11*, 309.
(35) Gupta, M. C.; Deshmukh, V. G. *Colloid Polym. Sci.* **1982**, *260*, 308.
(36) Gupta, M. C.; Deshmukh, V. G. *Colloid Polym. Sci.* **1982**, *260*, 514.
(37) Garozzo, D.; Giuffrida, M.; Montaudo, G. *Macromolecules* **1986**, *19*, 1643.
(38) Lyudvig, E. B.; Barskaya, I. G. *Dokl. Phys. Chem.* **1984**, *273*, 864.
(39) Barskaya, I. G.; Lyudvig, E. B.; Shifrina, R. R.; Izyumnikov, A. L. *Polym. Sci. U.S.S.R.* **1983**, *25*, 1491.
(40) Fischer, E. W.; Sterzel, H. J.; Wegner, G. *Kolloid Z. Z. Polym.* **1973**, *251*, 980.
(41) Vasanthakumari, R.; Pennings, A. J. *Polymer* **1983**, *24*, 175.
(42) Schindler, A.; Hibionada, Y. M.; Pitt, C. G. *J. Polym. Sci., Polym. Chem. Ed.* **1982**, *20*, 319.

MA970631M